

Influence of phase transitions on the second harmonic generation in metal nanoparticles

S. Achilli¹, M. Allione¹, A.M. Malvezzi^{2,a}, M. Patrini^{1,b}, A. Stella¹, P. Cheyssac³, and R. Kofman³

¹ INFN - Dip. Fisica “A. Volta” Università di Pavia, Via Bassi 6, 27100 Pavia, Italy

² INFN - Dip. Elettronica, Università di Pavia, Via Ferrata 1, 27100 Pavia, Italy

³ Laboratoire de la Physique de la Matière Condensée^c, Université de Nice Sophia Antipolis, 06108 Nice Cedex, France

Received 10 September 2002

Published online 3 July 2003 – © EDP Sciences, Società Italiana di Fisica, Springer-Verlag 2003

Abstract. In this work we use nonlinear optical properties of Ga nanoparticles monolayers of different average sizes embedded in dielectric matrices to investigate the liquid–solid phase transitions in these materials. Ga nanoparticles, formed by exploiting the partial wetting of liquid Ga over a SiO_x surface are irradiated with fs laser pulses from a Ti:sapphire source. The resulting Second Harmonic (SH) generated in the reflection and transmission directions is measured along the phase transitions by cooling the sample from 320 K down to liquid nitrogen temperature. Hysteresis cycles are observed in the nonlinear transmission, which exhibit a strong amplification from the solid to liquid values as compared to the linear optical results. A simple model for SH generation, based on Mie scattering calculations which includes the effect of surface plasmon resonance provides a fair key for the interpretation of the observed effects.

PACS. 78.66.Vs Fine-particle systems – 61.25.Mv Liquid metals and alloys – 42.65.Ky Frequency conversion; harmonic generation, including higher-order harmonic generation

1 Introduction

In the field of optoelectronics the nanostructured materials and, among them, aggregates of nanoparticles are attracting increasing interest. In fact, these systems show two important features. First, layers of metallic nanoparticles have been shown to have large nonlinear susceptibility due to the strongly enhanced fields localized at the constituent metal particles. This will be of great importance for the realization of optical logic circuitry and all-optical switches. Second, there is the possibility to grow them in an easy and low-expensive self-assembled way [1].

As it is well-known, second-harmonic generation (SHG) is forbidden in centrosymmetric media within the dipole approximation, but at an interface between different media this symmetry is broken [2]. In nanoparticles, the surface-to-volume ratio is greatly increased with respect to bulk materials, therefore high SH yield is expected. The nonlinear response can also be enhanced by the coupling of the incoming beam (or the generated SH beam) with other excitations in the medium like surface plasmon oscillations at the surface of metal nanoparticles [3]. Both these effects therefore establish in such media favourable conditions for an efficient nonlinear generation

of *e.g.* second harmonic radiation. Conversely, SHG can be conveniently used to investigate structures and properties of nanostructures [4]. Recently, nonlinear optical techniques have been used to analyze the spatial arrangement and the geometrical shapes of Ga nanoparticles [5].

In this work, the use of nonlinear techniques is extended to investigate thermodynamical properties of these systems. In particular, SH response induced by fs laser pulses is monitored across the liquid-to-solid phase transition of Ga nanoparticles on samples of average radii distributed over a wide interval. The results show hysteresis cycles for the SH signal across the phase transition. Most interestingly, the SH nonlinear transmission exhibit an amplification from solid to liquid values which is two orders of magnitude higher than the corresponding amplification of the linear case [6]. Besides the *per se* interest, these effects further stress the importance of SH generation as a useful tool for investigating nanostructured systems.

2 Experimental details

Ga nanoparticles are formed by evaporation-condensation (Vollmer-Weber mode) of high purity gallium on a dielectric substrate in ultrahigh vacuum. Metal particles are formed in the liquid state by a self-organization process

^a e-mail: malvezzi@ele.unipv.it

^b e-mail: patrini@fisicavolta.unipv.it

^c URA 190

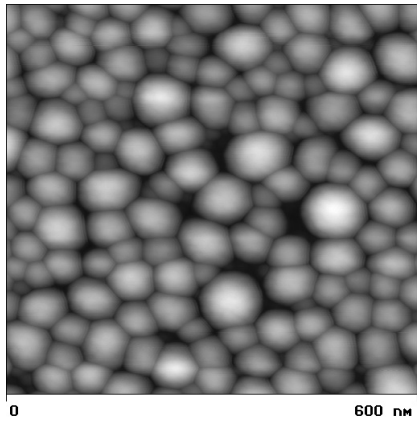


Fig. 1. Non-contact AFM image of a Ga nanoparticle sample characterized by equivalent thickness $d_M = 10$ nm.

and the substrate temperature is subsequently lowered until they are solidified. Details of the growing technique are given in reference [7]. Nanoparticles have a low-size dispersion ($\leq 20\%$) and an oblate spheroidal shape. They are grown on a 5 nm thin film of SiO_x , deposited by evaporation over a silica or sapphire substrate, and covered by another SiO_x layer which preserves particle shape and prevents chemical reactions due to air contact. The samples have an equivalent mass thickness d_M ranging from 1 to 200 nm. The equivalent mass thickness is defined as the thickness of the layer that would be formed if the evaporated material were uniformly distributed over the surface. The corresponding value of the mean radius of the particles was estimated by transmission electron microscopy (TEM) measurements on co-evaporated samples and was about twice d_M [8]. The size and shape of the particles have also been checked by means of an Atomic Force Microscope (AFM) and an image obtained on one of our samples of mean radius 20 nm is reported in Figure 1. Second harmonic generation was measured in transmission and reflection with a femtosecond Ti:sapphire laser at 810 nm, repetition rate 1 kHz, pulse duration 150 fs (setup A). The maximum pulse fluence on sample is $5 \times 10^{-3} \text{ J/cm}^2$ at the 0.9 mm diameter focal spot of the 4-m focusing lens used in the experiment. The SH signal is detected by a photomultiplier, after passing through a combination of color glass and interference filters to suppress the fundamental radiation. Measurements were also repeated in the 760–830 nm range with a femtosecond Ti:sapphire laser oscillator repetition rate 80 MHz, pulse duration 130 fs. The illuminated area was $\sim 30\text{--}40 \mu\text{m}$. In this setup (hereafter indicated as setup B) the peak fluence is several thousand times less than the previous case. However, it provides a higher average fluence to the sample. This imposes to reduce the duty cycle of the pulse train onto the sample in order to prevent excessive heat load on Ga nanoparticles.

3 Results and discussion

Nonlinear reflectance and transmittance R_{nl} and T_{nl} ($T_{nl} = I_T^{2\omega} / I_0^\omega$) measurements were performed on several

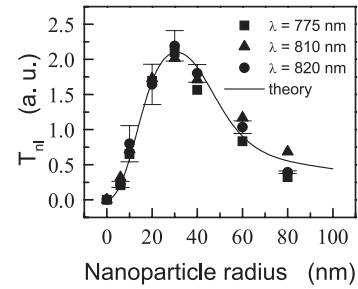


Fig. 2. SH transmittance signals for Ga nanoparticle samples of different d_M (*i.e.* different particle radii). The behaviour is the same also in reflection. Different symbols refer to different excitation wavelengths. The solid line is the result of the simulation with a nonlinear scattering model (see text).

sets of Ga nanoparticle samples at normal incidence (few degrees from normal direction in reflection). The measured SH signals from our samples show a strong dependence on the average particle. Both reflected and transmitted signals exhibit the same behaviour at room and at Liquid Nitrogen Temperature (LNT).

The measured signals show a broad maximum for $d_M = 15$ nm, *i.e.* for average nanoparticle radii of about 30 nm. The analysis of the linear absorbance spectra of the same samples reveals that for particles of this size the surface plasmon peak falls at the wavelength of our SH radiation, *i.e.* ≈ 400 nm. This coincidence suggests the origin of the SH enhancement as due to the resonance of the SH field with surface plasmon oscillations in the metal nanoparticles [6].

In order to further explore the role of the plasmon resonance in the SH signal we have performed measurements by changing the pump laser wavelength. In the experimental setup B the wavelength was then tuned in the range 760–830 nm. Figure 2 shows the T_{nl} results for a set of samples for $\lambda = 775, 810, 820$ nm pumping wavelengths. The dependence of the SH signal on wavelength appears very weak. In particular, the expected displacement of the maxima of the curves is almost unnoticeable, though consistent with plasmon resonance positions [6]. The results, however, are modified by (a) the finite bandwidth of the laser pump, which was measured to be ≈ 30 nm and (b) the size dispersion of the nanoparticles in our samples which amounts to $\pm 20\%$ of the nominal radius. These two occurrences limit the possibility of a fine resolution in the SH peak position *vs.* pump wavelength.

An attempt to model the enhancement of SH signals in resonance with surface plasmons has been pursued along the lines of reference [9] which uses a Mie representation of the nonlinear scattering mechanisms. These calculations are based on local enhancement of the electric field at the surface of the metal nanoparticles embedded in a dielectric medium. The parameters of such calculations are the complex refractive index of the metal and the effective index of refraction of the whole system in the Maxwell-Garnett approximation.

The results obtained for the SH response *versus* particle radius, using published values for the optical constants

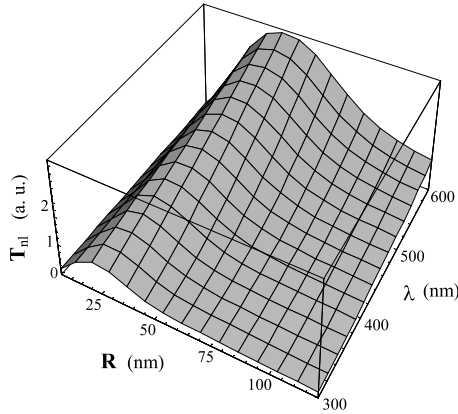


Fig. 3. SH transmittance for Ga nanoparticle samples of different particle radii as a function of the SH wavelength.

of liquid Ga and SiO_x , show in fact a broad maximum at ≈ 30 nm (solid line in Fig. 2). The simulations for the three pump wavelengths of the experiment are substantially coincident.

This model has also been used to evaluate the SH generated signals as a function of both SH wavelength and particle size. In Figure 3 the results of such a modelling is presented for SiO_x embedded Ga nanoparticles as a function of the SH wavelength ($300 \text{ nm} \leq \lambda \leq 600 \text{ nm}$) and particle size (up to $R = 120$ nm radii). The main features observed experimentally are qualitatively reproduced here. In particular, a line of maxima is obtained which extends towards increasing R 's and λ 's. Also, the intensity trend of the signal is reproduced, with values increasing with particle size. This model is showing its usefulness in the modelling of the nonlinear response of nanocomposite materials and is easily implemented in different situations as will be described below.

It is of some interest to measure the variation of the nonlinear properties of these materials across the solid-liquid phase transitions. In this respect, gallium appears an ideal candidate for such studies due to its low melting point (≈ 300 K in the bulk) and high nonlinear response as compared to other metals [10]. Therefore, SH signal has been collected while heating and cooling the samples for temperatures in the range LNT–320 K. The sample is kept in a cold finger cryostat driven by a temperature controller with a scan rate of 3 K/min while SH transmission at normal incidence is being continuously measured. Measurement runs start at $T = 320$ K in order to destroy the dimer structure of liquid α -Ga at room temperature [11]. The temperature is then decreased down to LNT and raised back to 320 K.

Figure 4 reports the results for such a measurement on a sample of average radius of 20 nm (carried out with the experimental setup A, data points averaged over 10 K). The results show a hysteresis cycle in the solidification-melting process. During cooling, quasi-constant SH generation is observed until 150 K where a sharp $\sim 30\%$ drop occurs. On the other hand, heating phase maintains the

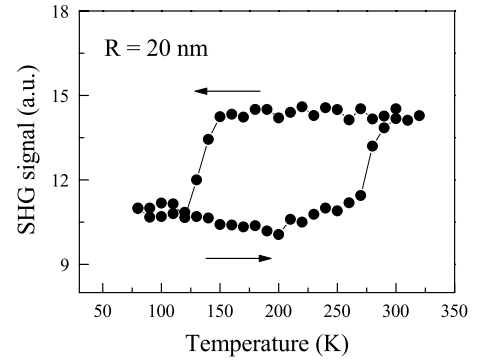


Fig. 4. Hysteresis of the SH transmission T_{nl} of 810 nm pulses as a function of sample temperature for a Ga nanoparticle sample with average radius 20 nm.

low SH values up to 270 K. A symmetric rise in SH is then observed which closes the cycle. This behaviour is typical of hysteresis cycles associated to the melting-solidification phase transition in nanoparticle aggregates. This has already been observed and described through linear optical measurements by other authors [12].

Similar hysteresis curves are observed in all the samples with additional features [6]. In particular, the maximum T_{nl} variation follows accurately the particle size dependence, with a maximum at $R \sim 40$ nm. Finer structures both during cooling and heating are observed superimposed to the main trend. These can be attributed to solid-solid phase transitions from different phases of metallic Ga [12,13]. Measurements were also performed with experimental setup B. Due to the unfavourable ratio between average and peak powers delivered on sample, SH signals obtained are more noisy and perturbed by the heavier thermal load.

Across the phase transition the T_{nl} values are amplified by 15–35%. It is interesting to note that the increase in the linear optical transmittance for these samples in correspondence of the solid-to-liquid phase transition, when detected, amounts to less than 0.5%. This specific sensitivity of SH radiation to the gallium phase may be explained as the results of the interplay of different mechanisms such as (a) the already stated large surface-to-volume ratio of these systems, (b) the strong dependence of the nanoparticle-matrix interface on the solid or liquid state of the gallium and (c) the already demonstrated predominance of the surface contribution with respect to bulk in SH generation [5]. The modelling procedure described above can be again used to estimate the amplification factor $H = I_l^{2w}/I_s^{2w}$ in the SH generation between solid and liquid Ga nanoparticles. The main task is to evaluate the polarizability of Ga nanoparticles in the two phases. By using literature data for the dielectric functions, the mass densities and the free electron densities in both phases a self-consistent estimate of $H = 2.4 \pm 0.5$ is obtained. This fairly approaches our experimental values of $H = 1.4 \pm 0.2$ (by considering the error bars) obtained with SH signals at 300 and 77 K.

4 Conclusions

SH generation has been efficiently observed in monolayers of Ga nanoparticles. The signal has been studied on samples of different average sizes showing large variations with a strong maximum. This fact indicates the central role of the coupling of the incoming radiation with surface plasmon oscillations. The maximum has been interpreted as the effect of resonance of such a coupling. The same effect has also been investigated by changing the pump wavelength in the 775–820 nm range, obtaining similar results. Also, the same behavior is observed at different temperatures down to LNT.

Through second-harmonic generation we have also observed a hysteresis curve for Ga nanoparticles across the solid–liquid phases. Strong amplitude variations of the cycles with particle size have also been observed. Moreover, fine structures superimposed to the main hysteresis behavior have been noticed. Their appearance may be interpreted as due to solid–solid phase transitions of metallic gallium. An amplification factor of two orders of magnitude is observed in the ratio of the melting-induced enhancement of the SH signal with respect to the linear response at the same wavelength.

The overall data have been interpreted within a model based on nonlinear Mie scattering of the pump radiation and subsequent SHG. For both size and temperature dependence the analysis here developed stresses the key role of parameters like mass density, dielectric function and free-carrier concentration, in determining the SH behavior.

We acknowledge financial support from Progetto di Ateneo “Nuovi materiali nanostrutturati” by the University of Pavia.

References

1. For a review, see *e.g.* *Handbook of Nanostructured Materials and Nanotechnology*, edited by H.S. Nalwa (Academic Press, S. Diego, 2000), Vol. 4
2. D. Ricard, P. Roussignol, C. Flytzanis, *Opt. Lett.* **10**, 511 (1985)
3. A. Brysch, G. Bour, R. Neuendorf, U. Kreibig, *Appl. Phys. B* **68**, 447 (1999)
4. O.A. Aktsipetrov, P.V. Alyutin, A.A. Fedyanin, A.A. Niculin, A.N. Rubtsov, *Surf. Sci.* **325**, 343 (1995); M. Simon, F. Trager, A. Assion, B. Lang, S. Voll, G. Gerber, *Chem. Phys. Lett.* **296**, 579 (1998)
5. A.M. Malvezzi, M. Patrini, A. Stella, P. Tognini, P. Cheyssac, R. Kofman, *Eur. Phys. J. D* **16**, 321 (2001)
6. A.M. Malvezzi, M. Allione, M. Patrini, A. Stella, P. Cheyssac, R. Kofman, *Phys. Rev. Lett.* **89**, 087401 (2002)
7. E. Sondergard, R. Kofman, P. Cheyssac, A. Stella, *Surf. Sci.* **364**, 467 (1996)
8. P. Tognini, A. Stella, P. Cheyssac, R. Kofman, *J. Non-Cryst. Solids* **249**, 117 (1999)
9. T. Müller, P.H. Vaccaro, F. Balzer, H.-G. Rubahn, *Opt. Commun.* **135**, 103 (1997)
10. G.T. Boyd, T. Rasing, J.R. Leite, Y.R. Shen, *Phys. Rev. B* **30**, 519 (1984)
11. R. Kofman, P. Cheyssac, R. Garrigos, *Phase Trans.* **24-26**, 283 (1990)
12. A. Defrain, *J. Chim. Phys.* **74**, 851 (1977)
13. A. Di Cicco, *Phys. Rev. Lett.* **81**, 2942 (1998)